Design of a wiper as compliant mechanisms with a monolithic layout

Antonio Pantano*, Gemma Minore, Giovanni Carollo

Dipartimento di Ingegneria, Università degli Studi di Palermo, 90128, Palermo, Italy
* Corresponding Author / E-mail: antonio.pantano@unipa.it

Abstract
The increasingly important need to design simpler structures, reducing the number of constituent components, has motivated the approach outlined in this paper which proposes an effective re-engineering example of a product belonging to the automotive industry, combining the advantages offered by the compliant mechanisms with production opportunities linked to the use of additive manufacturing. Take advantage of compliant mechanisms makes it possible to significantly improve the component's production phase, leading to undoubted benefits on the supply chain and on product's time to market, benefits made possible by exploiting the outstanding characteristic of additive manufacturing to produce already assembled multi-material structures. The performances of the innovative monocomponent wiper designed here were compared, with the help of FEM simulations, with those of the component made in the traditional way and with those of the only other existing single-component frame of which we have news, the one patented by the US company Flexsys, obtaining satisfactory results both in terms of weight reduction, and for the best pressure distribution at the wiper / glass interface, and in terms of maximum stress reduction.

Keywords
Compliant mechanisms – Monocomponent – Wiper – Additive Manufacturing

1. Introduction

The term compliant mechanism refers to jointless structures that allow the transfer of energy from an input port to an output port through its elastic body deformation without the presence of any rigid connection between several parts [1-2]. Rigid areas, which must resist the application of the load, must be differentiated from flexible areas that must allow movement. The applied input force is transferred to the exit door in a manner similar to that of the corresponding rigid mechanism, the only difference being that in the compliant mechanism part of the energy is stored in the form of deformation energy. One of the most important advantages of replacing a rigid mechanism with the corresponding compliant version consists in drastically reducing the quantity of components that make up the system, according to the Part Count Reduction aim, often allowing the creation of a single component mechanism with a monolithic design. Pursuing the part count reduction goal would also make it possible to simplify inventory management, an essential aspect in a global supply chain perspective, as well as to reduce the possibility of making mistakes during assembly. Other advantages of compliant mechanisms have been shown in reducing weight, backlash, wear, assembly time and maintenance, increasing precision, reliability and performance, and simplifying manufacturing processes, as well as eliminate friction. Compliant mechanisms offers unique possibilities in a wide range of application fields, for example: grippers, manipulators and sensors with macro, micro or nano size scale able to achieve ultrahigh precision accuracy [3-9]; biological cell manipulation [10-11]; optical fiber alignment [12-13]; MEMS [14]. The purpose of this paper is to offer a concrete example of re-engineering of a product traditionally made up of a large number of components and joining elements, with the aim of making it a single-component structure using the aid of additive manufacturing. Such a philosophy could be applied to a varied number of mechanisms, but in the specific case it was decided to choose a component of use in the automotive sector. Indeed, a critical aspect in this field is linked to the effective integration within the same structure of mechanical, electrical and electronic systems. In this

perspective the potential of additive manufacturing to realize complex hollow structures and reticular structures is particularly advantageous, allowing the reduction of dimensions and consumptions. Moreover, manufacturers are increasingly engaged in speeding up the assembly phase, above all for complex systems rich in components such as the automobile, as well as in the search for new high-performance lightweight materials. Based on these considerations it was decided to focus attention on the chassis of a motor vehicle wiper, a product used by all of us every day, essential for the safety of any car and which, despite its apparent simplicity, is made up of many components and therefore characterized by a rather complex assembly phase. It is therefore worth trying to exploit new available technologies, such as additive manufacturing, to redesign its structure to create a product that can be produced as a single component, greatly simplifying the production phase and also reducing weight.

2. Wiper operation and features: existing models and re-engineering approach

2.1 Traditional multicomponent wiper

To allow an effective re-engineering of the component, prior to the design phase it was necessary to analyze the functioning of a traditional windscreen wiper, in order to understand the essential aspects to be used as a basis for the design of the innovative frame. The structural components that allow the pressure required for correct operation to be applied to the windscreen are listed below: the blade, which has the function of removing water from the windshield, is made up of rubber internally reinforced by two curved metal vertebrae to promote the most uniform pressure distribution possible; the frame, which must support the blade, is formed by metal arches connected to each other by hinges; the arm, usually made of galvanized steel, which applies to the frame the necessary force to make the rubber adhere correctly to the windshield, allowing the intermittent movement generated by the electric motor to which it is connected. The purpose of the windscreen wiper is to ensure adequate visibility conditions for the driver by cleaning the windshield. The latter has a surface with variable radius of curvature on which the wiper must adhere by flexing through hinges connecting the metal arches of the frame. The design will therefore refer to the most critical configuration, i.e. that in which the radius of curvature is greater. A fundamental requirement of the component is to apply a pressure as uniform as possible on the contact surface with the windshield, avoiding undesirable deviations that would lead to insufficient cleaning, for example in particularly heavy weather conditions. Exposure to atmospheric agents must also be taken into particular consideration when choosing the material, which must exhibit constant properties in the temperature range between 5 ° C and 40 ° C, as indicated by European Union legislation. The vehicle for which the innovative chassis was developed is the Fiat Panda 2nd series and specifically it was decided to analyze and redesign the chassis of the larger of the two front windscreen wipers. In order to perform a more accurate analysis of the operation of a traditional chassis of this type, a specific model was purchased for the vehicle in question. It is an aluminium frame, with one input point and eight output points, produced by the Lucas company, with a brush length of 550 mm (Figure 1), consisting of a main arch, two secondary arches and four outer arches.

***Figure 1**. Example of conventional frame for Fiat Panda 2nd series*

Following precise measurements made using a digital caliper, a three-dimensional model was created using Autodesk Fusion 360 software, necessary for comparing the frames performance through finite element analysis (Figure 2). In order not to weigh down the simulations unnecessarily, although the rubber blade has a very particular cross section, it was decided to model it considering a rectangular section of 8mm * 10mm, since this geometry has no relevant influence on the comparison between the various frames. For the same reason the surface of the windshield was only partly modeled, considering a width of 12 mm.

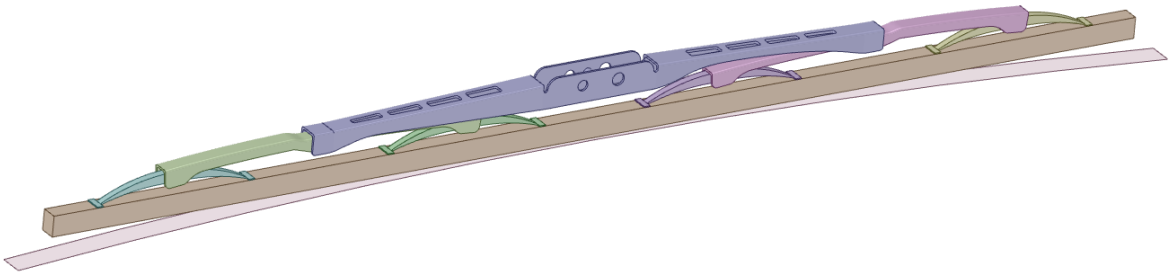

***Figure 2**. CAD model of the traditional wiper and windshield surface*

2.2 Single-component wiper: Flexsys frame

In addition to the traditional component, for a performance comparison it was analyzed the only other existing single-component windscreen wiper, patented by the US company Flexsys that improved the conventionally used structure so that the input force from the arm was theoretically divided as equally as possible into the eight contact points between the frame and the blade. The Flexsys frame scheme is in fact based on the repetition of triangular elements that divide an input force into two output forces (Figure 3), which are differently distributed according to the length of the sections l_1 and l_2, in accordance with the following equations in Figure 3. [15]

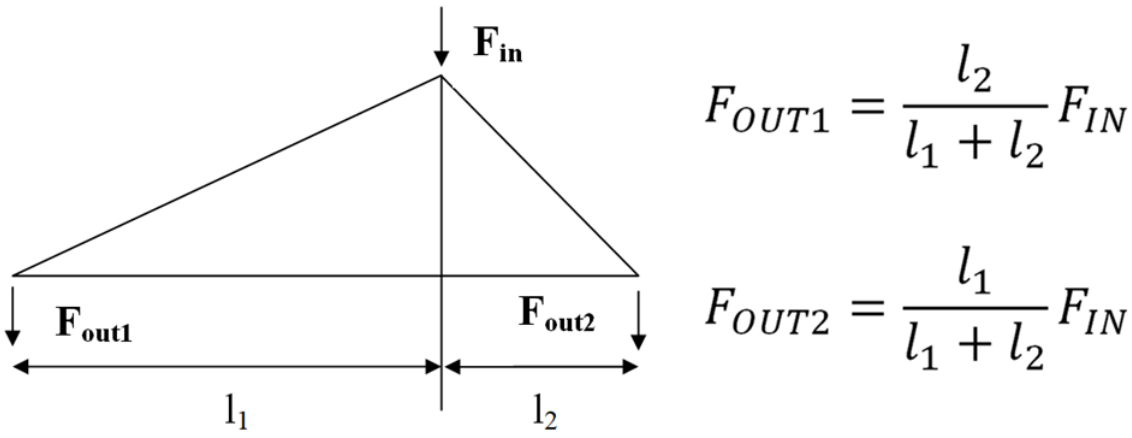

***Figure 3**. Input - output force diagram and mathematical equations*

The theoretical model, obtained by repeating the illustrated scheme along different levels, in fact leads to a uniform distribution of the input force towards the contact points shown in Figure 4 (only half structure is represented, since it's symmetrical).

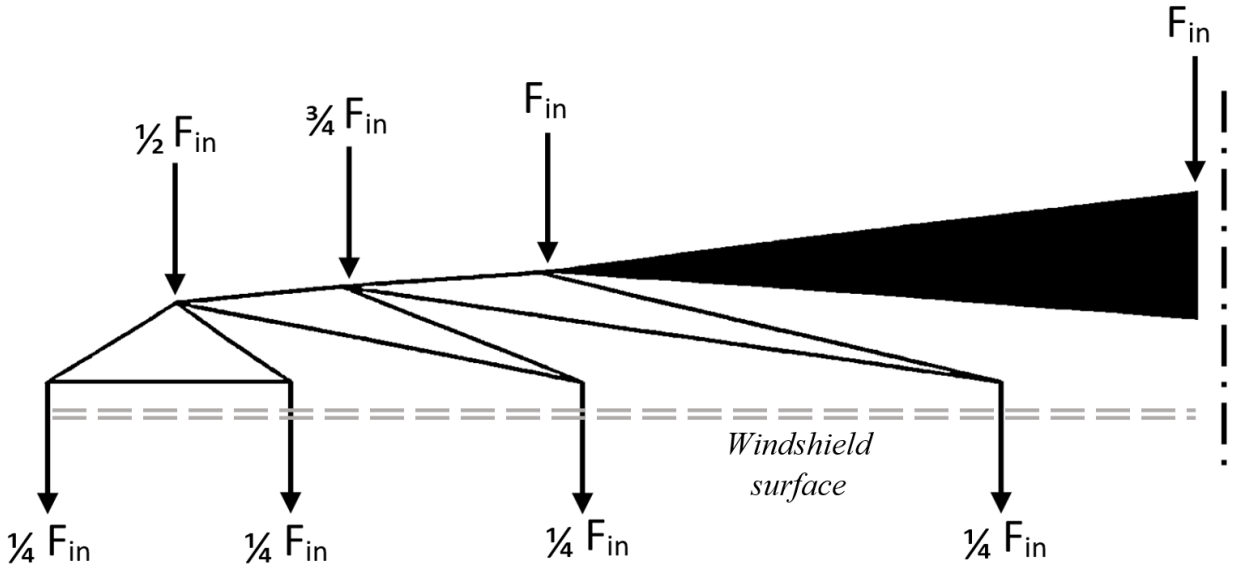

***Figure 4**. Preliminary theoretical geometry of the Flexsys frame and force distribution (only half frame is represented)*

This model was subsequently refined using topological optimization, obtaining the final frame which we have modeled respecting the sizing information present in the relative patent. Unlike the traditional frame, which initially keeps the blade in a rectilinear position to subsequently bend it by applying force from the arm, the single-component Flexsys frame was produced in such a way as to give a certain initial curvature to the blade, which is then accentuated by the application of force, allowing it to adapt to the curvature of the windscreen during the various operating phases. For this reason the blade in the Flexsys frame has been modeled with an initial curvature equal to that of the frame but with the same section previously used for the traditional frame (Figure 5). The American company has chosen to produce the frame by injection using the PBT-GF30 thermoplastic polyester resin, 30% reinforced with glass fiber, whose main mechanical properties are shown below (Table 1).

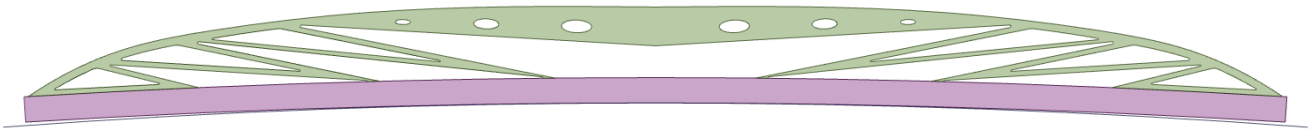

***Figure 5**. CAD model of the Flexsys frame and windshield surface, front view*

Mechanical properties				***Thermal properties***	
Density [kg/m^3]	Young modulus [MPa]	Ultimate tensile strenght [MPa]	Maximum deformation [%]	melting temperature [°C]	HDT [°C]
1520	9600	130	2.5	225	205

***Table 1**. Mechanical and thermal characteristics of the PBT-GF30 resin (Crastin) produced by DuPont*

2.3 Design of an innovative monocomponent wiper

Once analyzed the essential characteristics required to the product, an attempt was made to introduce substantial innovations in the structure that would allow it to compete in the market, guaranteeing performance at least equal to the innovative Flexsys frame but possibly with less weight. In fact, during product re-engineering, to take as much advantage as possible from the use of compliant mechanisms

was a fundamental aspect, supported by the considerable production opportunities granted by additive manufacturing. In the design of a component, the first aspect to be evaluated is the choice of the material to be used. Therefore, materials such as steel or aluminum were rejected because, despite their increasing use in additive manufacturing, the metal 3D printing process still has significant costs, justifiable for example in the aerospace and biomedical field where large-scale production is not required, vice versa for this kind of component the use of thermoplastic polymers has been preferred for their low cost and for their effective use in additive manufacturing. The latter were compared on the basis of parameters such as resistance to heat, UV rays and humidity, but also tensile strength, stiffness and fatigue strength. In particular, after excluding ABS, PLA, polypropylene and polystyrene, the research focused on polyethylene and nylon. The former, although possessing a greater Young modulus, useful for increasing the rigidity of the structure, also has a Heat Deflection Temperature (HDT) lower than nylon, therefore the material loses consistency deforming at a lower temperature than nylon. Therefore it was decided to use NYLFORCE CF, that is carbon-reinforced nylon, whose main properties are shown below in Table 2.

Mechanical properties			***Thermal properties***			
Density [kg/m^3]	Young modulus [MPa]	Ultimate tensile strenght [MPa]	Melting temperature [°C]	HDT [°C]	Max temp. of use long period [°C]	Max temp. of use short period [°C]
1000	6000	100	180	155	90 – 120	150

Table 2*. Mechanical and thermal properties of NYLFORCE CF produced by Fiber Force Italy*

Subsequently it was necessary to decide whether the initial undeformed configuration of the frame had to be with a straight blade (similar to the traditional frame) or curved (as in the Flexsys frame). After evaluating some configurations, the first hypothesis was excluded because a straight blade would have required a flexible mechanism with concentrated compliance, that is with very thin flexible joints which would have neither ensured the resistance of the system nor allowed to obtain sufficient pressure at the ends of the blade. It was therefore decided to design an already curved frame in its undeformed condition, whose curvature radius could increase following the application of the load and then coincide with the surface of the windscreen. To simplify the identification of the optimal configuration, the structure was assigned a constant thickness of 12 mm, so as to be able to exclusively evaluate the geometry of the structure on the plane. Unlike the Flexsys frame, based on the repetition of the triangular elements that subdivide an input force into two output forces, the structure of the innovative frame here proposed is inspired by the logic of compliant mechanisms, which simultaneously conciliate, within the same structure, the presence of rigid areas, designed to resist the application of the load, and of flexible areas that allow the movements necessary for the component to function. In this perspective, each portion of the mechanism plays a fundamental role since it is able to influence the behavior of the entire structure.

Although the starting geometry was conceived in broad lines by the authors, in order to determine the optimal configuration, a parametric Cad model was initially created, containing the main geometric parameters relating to the position, thickness and inclination of the various elements. Subsequently, using this parameterized model, a series of Fem analyzes were carried out using the Adaptive Single Objective Optimization Method, a mathematical optimization method based on gradients and response surfaces. The several geometric parameters were therefore varied within a certain range of admissible values in each optimization analysis, and by setting the maximum Von Mises stress as an objective

function to be minimized, it was possible to obtain the most suitable geometric parameter values in order to identify the optimal configuration of the structure subjected to the least possible stress. In order to provide the reader with further general indications that could be followed for a first approach to the design of this kind of structure, below will be highlighted although approximately some details on the reasoning that motivated some design choices related to the final configuration of the frame, choices supported by the results of numerical optimization analyzes.
Considering the constraint, linked both to the direction and to the application area of the force produced by the arm on the frame, it was decided to model the central area of the structure, i.e. the one in the vicinity of which the load is applied, so that it can be as rigid as possible without, however, resorting to the use of a thick beam such as that present both in the traditional component and in the Flexsys frame. At the same time an attempt has been made to make the outermost areas sufficiently flexible so as to adequately follow the curvature of the windscreen during the various operating positions and apply sufficient pressure on it to maintain contact even in the most severe grip conditions. The following is a simplified outline of the final configuration that has been identified (Figure 6). The transmission of the input force to the entire structure occurs mainly by means of the element 1 while the elements 4 and 5 transfer the pressure to the blade and allow to locally increase the stiffness, both coming together at the same point. In fact, it is necessary to consider that the frame and the blade, as seen in the frames on the market, are not rigidly connected but through prismatic guides that allow the blade to slide along the axis of the guide, blocking the movement in the perpendicular direction instead. Therefore, if for example the element 4 were not present, the application of force on the system would lead to an excessive sliding of the element 5 on the brush, which on the one side would cause a sort of local squashing of the mechanism, on the other the application of too low pressure on the brush in the central area. The position and inclination of the elements 4 and 5 have therefore been defined in such a way as to find the right balance between sliding and application of the correct pressure value. In fact, if the values of the angles α and β approach 90° (Figure 7), the pressure applied to point A increases, but at the same time the blade is not allowed to slide adequately along the prismatic guides, thus hindering the correct operation of the wiper.

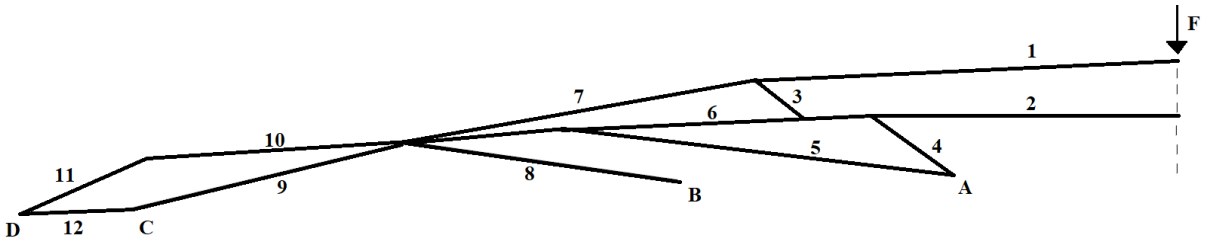

Figure 6*. Scheme of the innovative frame with relative numbering of the components (only half structure is represented, since it is symmetrical)*

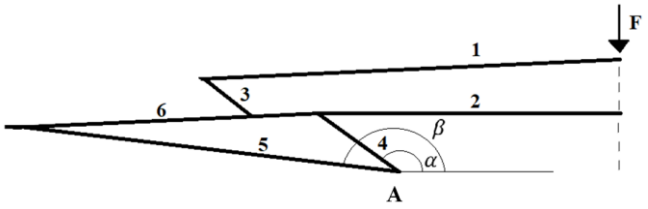

Figure 7*. Diagram of block 1-2-3-4-5-6, with angles α and β highlighted*

The positioning of the element 2 was instead established so as to confer greater rigidity close to the load application area. Therefore, maintaining the geometry shown in Figure 7 constant, mainly

designed to resist the application of the load by giving stiffness to the structure, various solutions for modeling the ends of the frame were examined. The position of the element 7 is essential since it acquires a similar role to that played by the element 1, simultaneously transmitting the input force towards the blade both through the element 8 and through the system of elements 9-10-11-12. For the definition of the inclination of the elements 8 and 9, the same reasoning made previously for the elements 4 and 5 is valid, in fact also in this case the balance between application of the pressure and sufficient sliding of the blade along the prismatic guides has been sought. A compromise was also necessary in relation to the positioning of the element 3, since if on the one side its displacement towards the left allows a better transfer of the load from the central area to the peripheral area avoiding excessive stress on the elements 4 and 5, on the other side, the aforesaid displacement would reduce the pressure applied in the central part of the blade, with the risk also of having the elements 1 and 2 collide with each other during operation. The evolution between the various configurations of the conceived structure was supported by a conspicuous series of numerical simulations through finite element analysis that finally allowed to identify the most suitable conformation to distribute the load on the blade (Figure 6). Further information on this frame, its weight and its performance will be shown below, compared with those of the conventional frame and the Flexsys frame.

3. Performance comparison: numerical analyses configuration and results

In order to effectively compare the three different versions of frames described above it was necessary to simulate the behavior of the structures through finite element analysis, since the theoretical assumptions about their operation may deviate from the actual performances being the latter influenced by the actual shape and size of the components. Initially, the various assumptions underlying the numerical simulations aimed at comparing the performance of each frame will be described.

2.1 General parameters of the numerical model

In order to faithfully simulate the interaction between the chassis and the windscreen, based on field measurements in combination with the use of the vehicle's blue prints, it was possible to reproduce the geometry of the windscreen of the chosen vehicle (Fiat Panda 2nd series) obtaining a CAD model to be used for numerical simulations. The most critical configuration of operation, i.e. the one in which the radius of curvature is greater, after an analysis of the curvature radius of the surface was found to be the rest position of the wiper in which the component also spends most of its useful life in deformed condition, with the risk of undergoing permanent deformation in the event of an uneven pressure distribution. Following a series of measurements, the value F_i of the force exerted by the arm towards the frame was obtained, confirmed also by data in the literature [16] : $F_i = 10.79$ N.

The main goal of the simulations was to identify the pressure distribution at the rubber-windscreen interface, the displacements and the maximum stresses for each of the frames under examination.

The FEM analyzes were conducted by modeling the chassis components using brick elements, i.e. three-dimensional quadratic elements at 20 knots, each having 3 degrees of freedom relative to the displacements in the three directions, in addition, to create an efficient mesh even in areas with complex geometry, quadratic tetrahedral elements have also been used. For the surface of the windshield instead, shell elements have been exploited, having 4 nodes with each 6 degrees of freedom, i.e. the displacements in the three directions and the rotations around the three axes. Since the bodies interact with each other, it was also necessary to use contact elements. The materials constituting the three bodies to be modeled, being isotropic, can be characterized essentially through the Young's modulus and the Poisson's ratio (Table 3).

Material	Conventional frame Aluminum	Flexsys frame PBT –	Innovative frame Nylforce CF	Blade rubber	Windshield Glass

		GF30			
Young modulus [MPa]	71000	9500	6000	7.6	8700
Poisson ratio	0.33	0.42	0.42	0.49	0.25

Table 3*. General summary of material properties*

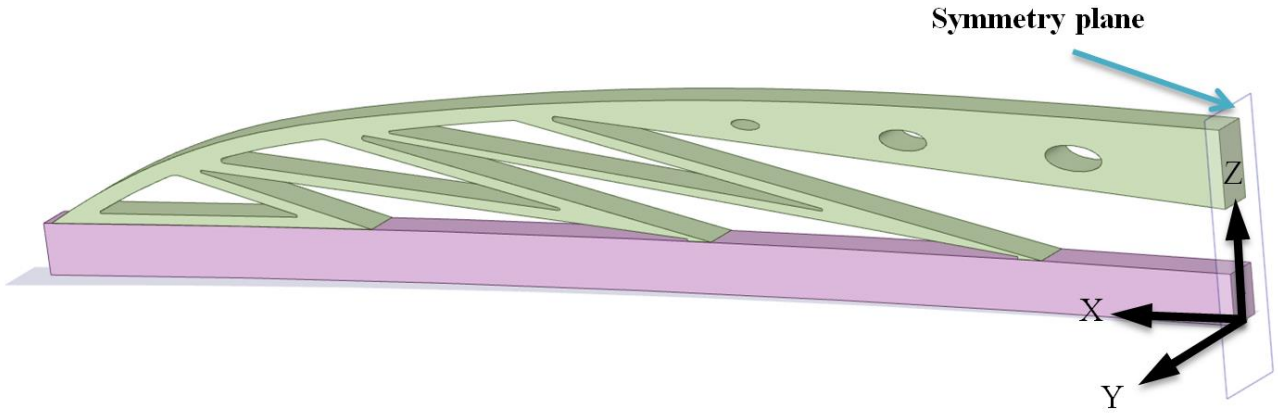

Figure 8*. CAD model of the Flexsys frame, representation of half structure, i.e. of that actually analyzed and of the corresponding symmetry plane*

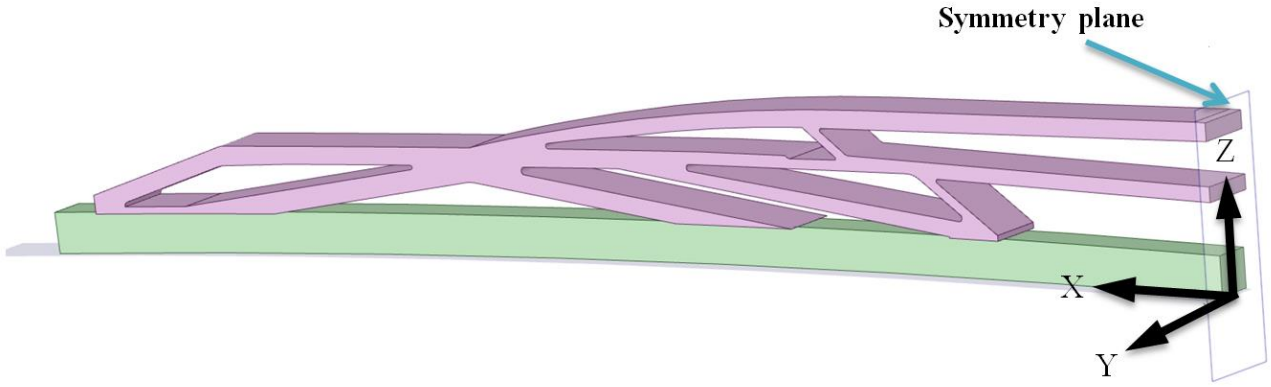

Figure 9*. CAD model of the innovative frame, representation of half structure, i.e. of that actually analyzed and of the corresponding symmetry plane*

To reduce the computational load required by the simulations, it was possible to exploit the geometric symmetry conditions of both monocomponent frames, analyzing only half of them (Figure 8 and 9), however this simplification was not possible for the traditional frame due to the asymmetry of the main arch. To describe loads and constraints more effectively, it is appropriate to define the reference system adopted: X axis coinciding with the longitudinal axis of the rubber, Y axis coinciding with the transversal axis of the rubber (along its width), Z axis coinciding with the transversal axis of the rubber (along its height). In order to assess which of the three frames is able to exert pressure on the windshield as evenly as possible, a first type of analysis was performed (indicated below with "Contact pressure analysis") considering the wiper in its rest condition, in which only the force coming from the arm is applied to the frame to allow the blade to adhere to the windshield. Another important aspect to ensure the correct functioning of the windscreen wiper is to check the flexural stiffness of the frame, so it was necessary to simulate, in the presence of friction, the behavior of the two single-component

structures, consisting of less rigid materials than the traditional frame, applying in addition to the force, even a shift in the Y direction. This kind of analysis will be referred to as "Flexural stiffness analysis" and will be performed exclusively for single-component frames.

2.2 Definition of contact conditions, boundary conditions, constraints and loads

2.2.1 Contact pressure analysis

In order not to introduce singularity in the simulations, the only force present F_i was not applied punctually but through an equivalent pressure uniformly distributed on a delimited area. In each simulation performed, the surface of the windshield has been deprived of any degree of freedom, while it was necessary to constrain the different frames differently. Specifically, in the conventional frame, in order to avoid rigid displacements between the different arches, the displacement in the Y direction was blocked on all surfaces with positive normal Y, while each degree of freedom was blocked on a small area in the middle of the blade. Besides, to effectively simulate the connection of the conventional frame to the arm, the displacements in the X and Y direction were blocked on the same area where the pressure was applied. Instead, in the two single-component frames, of which only half structure was analyzed exploiting the geometric symmetry conditions, only the displacement in the Y direction of all the areas lying on the YZ symmetry plane has been constrained, reproducing in this way the presence of the other half of the frame. As previously mentioned, the frame and blade are not rigidly connected but through prismatic guides (here for simplicity not shown geometrically) whose action has been simulated by imposing a "No Separation" type of contact that allows the sliding of the surfaces in the tangential direction while preventing their separation in the normal direction. The same kind of contact was also used in the surfaces of the connecting hinges between the arches present in the traditional frame. Given the low influence of friction between the blade and the windscreen in this first type of analysis, the sliding of the rubber in the Y direction is in fact insignificant, the contact between these two elements has been set as "Frictionless" allowing the sliding both tangentially and along the normal surfaces.

2.2.2 Flexural stiffness analysis

In the same area where the arm applies the pressure on the frame, a 10 mm displacement was imposed in the opposite direction to the Y axis. In addition to subtracting every degree of freedom from the surface of the windscreen, it has been constrained also the rotation around the 'X axis of a small surface of the frame with normal negative Y, adjacent to the load application area, with the aim of simulating the connection between the frame and the arm, which avoids precisely the rotation of the frame around the X axis during motion. Having to evaluate, in this second type of analysis, the flexural stiffness of the two single-component frames, it was also necessary to consider the effect of the friction between the blade and the windscreen, setting between them a "Frictional" type contact with friction coefficient $\mu = 0.5$ corresponding to the maximum friction value in wet conditions, as confirmed by data in literature [17]. In this case, moreover, the contact between the frame and the blade has been modeled as a "Bonded" type, preventing both the detachment and the relative sliding between the two surfaces, since otherwise allowing relative sliding would not have faithfully reproduced the behavior of the structure by not allowing load transfer from the frame to the blade.

2.2.3.Numerical analysis settings

In all the simulations carried out and for all the components modeled, the mesh used to compare the results was obtained following a convergence analysis procedure considering both the maximum equivalent Von Mises stress and the contact pressures. Initially, in fact, a uniform mesh was generated, progressively thickened in the areas of connection, of high curvature and of stress concentration up to obtaining stable values of pressure and equivalent stress. Furthermore, the presence of at least two

elements along the thickness in each area of the structure has been ensured. Both types of analyzes performed are static structural. The only external load present in “Contact pressure analysis” was applied in a single load step, with a different number of substep for each frame, determined through a convergence analysis. In the “Flexural stiffness analysis”, two load steps were required, in the first the pressure was applied in both single-component frames while in the second the displacement was imposed using 50 substeps. The presence of non-linearity in both analyzes, due to the use of the "Frictionless" or "Frictional" contact, made it necessary to exploit the Newton - Raphson iterative method of the "Full" type in “Contact pressure analysis”, and of the "Unsymmetric” type in the “Flexural stiffness analysis”, option recommended in the latter case for the use of a friction coefficient greater than 0.2. Finally, the formulation used to simulate contact in all frames is the "Augmented Lagrange" type.

2.3 Results: Contact pressure analysis

The performances of the three frames will be compared, describing for each frame the pressures distribution, the equivalent Von Mises stress and the displacements. Considering initially the traditional frame, the stress state has modest values, generally lower than 7.6 MPa and reach a maximum of 68.4 MPa in the area with a lower thickness, quite far from the aluminum ultimate tensile stress. Despite the asymmetry of the main arc, both the displacement trend (Figure 10) and the pressure distribution are symmetrical with respect to the YZ plane.

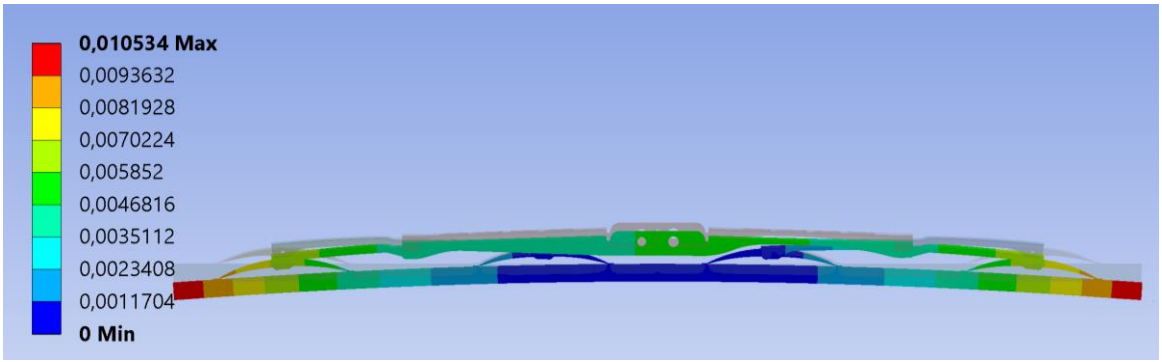

***Figure 10**. Comparison between undeformed (gray) and deformed configuration of the traditional frame, front view*

Considering half structure, the four areas with significant pressure have almost the same extension and correspond to the contact points between the frame and the blade. The maximum values reached by the displacement and the pressure are respectively 10.5 mm (at the ends of the frame) and 22729 Pa (in the central area of the blade). Both for the Flexsys frame and for the proposed innovative frame, as these components are symmetrical with respect to the YZ plane, the results are relative only to half of the modeled structure. In the Flexsys frame the greater displacements occur at the end of the blade and near the area where the load is applied to the frame (Figure 11), reaching a maximum value of 1.3 mm.

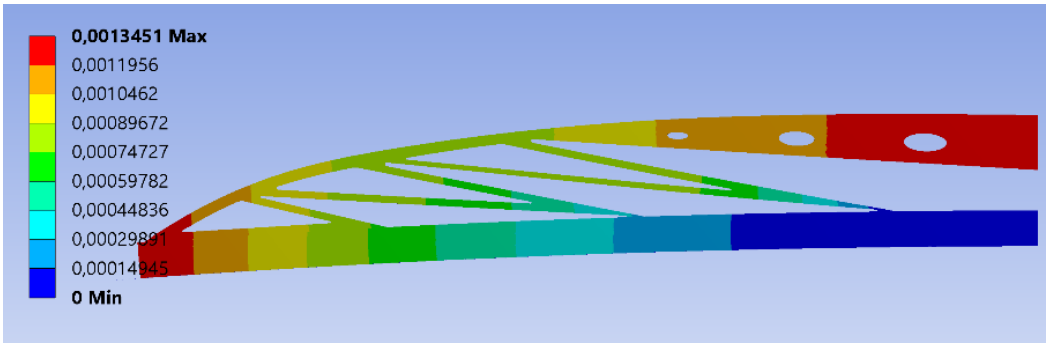

***Figure 11**. Total displacement of the Flexsys frame, front view*

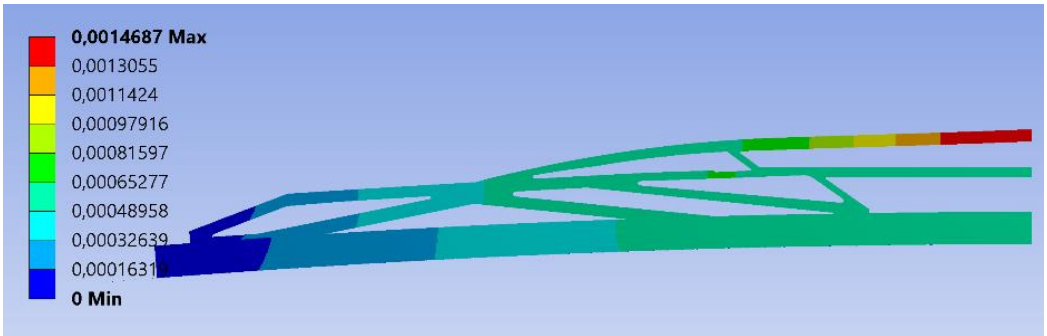

***Figure 12**. Total displacement of the innovative frame, front view*

Also in this case the stress state is not particularly heavy, remaining below 5 MPa except in the central contact area between the frame and the blade, in which it reaches 23.2 MPa, a stress much lower than that of tensile strength of the material equal to 130 MPa. The pressure on the Flexsys blade is distributed mainly on three areas which, unlike the traditional frame, do not possess the same extension or the same trend, since the largest area is at the end reaching a pressure of 20000 Pa while in the central zone, with a smaller area, a maximum pressure of 27487 Pa is reached. Considering finally the results relating to the innovative frame and first of all the trend of total displacements (Figure 12), a single zone with relevant displacements, in which a maximum of 1.5 mm is reached, coinciding with the beam on which the input load is applied. The stress state does not show any criticality even in this frame, remaining below 3.7 MPa and reaching the maximum value of 16.9 MPa in the connection area between the main beam and the rest of the structure. From the analysis of the pressure generated on half of the frame, it is possible to detect the presence of a small area at the end with low pressures and of three main areas rather similar in terms of extension and pressure distribution, where a maximum of 16547 Pa is reached.

2.4 Results: Flexural stiffness analysis

The application of the 10 mm displacement, in addition to the aforementioned pressure, leads the Flexsys frame to move almost rigidly in the imposed direction, since the displacements have values between 10 mm and 8.3 mm. The flexural behavior of the frame is effectively shown in the lateral view of the deformed structure (Figure 13a) compared with its undeformed condition, from which emerges the tendency to partially rotate around the X axis, an aspect that can be improved by increasing the width or using a material with a higher Young's modulus. Regarding the stress condition of the Flexsys frame, even in this flexural stiffness analysis the stress remain low, below 6.7 MPa, but the additional stress due to the imposed displacement, leads to the increase of the maximum stress up to 60 MPa which was reached, as in the previous analysis, in the same connection area between the frame and the blade. Also in the innovative frame the imposed displacement determined an almost totally rigid movement of the structure but with a flexural stiffness slightly lower than the Flexsys frame, where 8.3 mm displacement values were reached at the ends while in the innovative frame is reached 7.9 mm in the same area (Figure 13b).

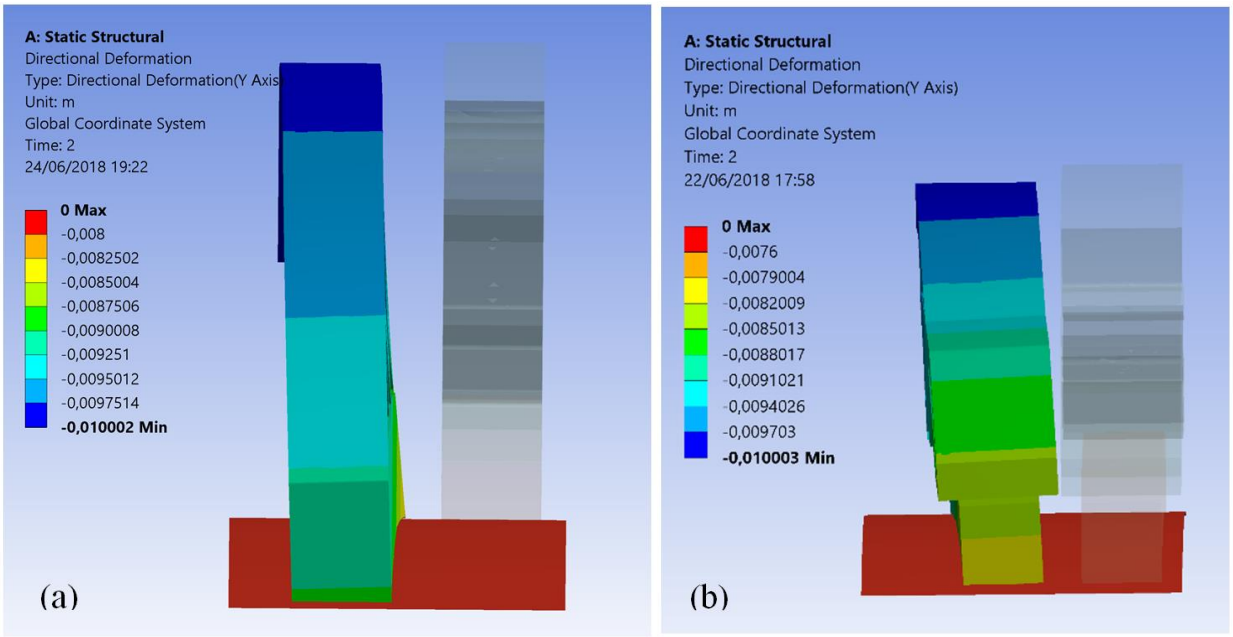

***Figure 13**. Total displacement in the Y direction, compared with the undeformed configuration (in gray), of the Flexsys frame (a)(amplified by a factor of 1,3) and of the innovative frame (b)(amplified by a factor of 1,5)*

The stress state, on the other hand, is even less burdensome than the Flexsys frame, in fact generally no stress exceeding 2.6 MPa occur, except in the area of the beam where the load is applied, in which they reach a maximum value of 23.4 MPa, however far from the ultimate tensile strength of the Nylforce CF.

2.5 Considerations on the compared frames

To effectively evaluate which of the three frames is able to redistribute the input load more evenly, the graphs of pressure trends along the longitudinal axis will be analyzed below for each of them. For all frames, the areas with relevant pressure values were numbered in ascending order starting from the end of the blade towards the centerline and furthermore for each area the pressure values of the knots located in the blade axis were plotted according to the abscissa X. In each graph, the first significant pressure value detected was placed at the origin to better highlight the extension along the X axis of each numbered area. The pressures trends and the relative graphs shown below, considering the conditions of symmetry, refer to the half of each frame. Analyzing the conventional frame first, there is a bell-shaped pressure pattern in the four main areas, symmetrical in area 3 and asymmetrical in the others (Figure 14).

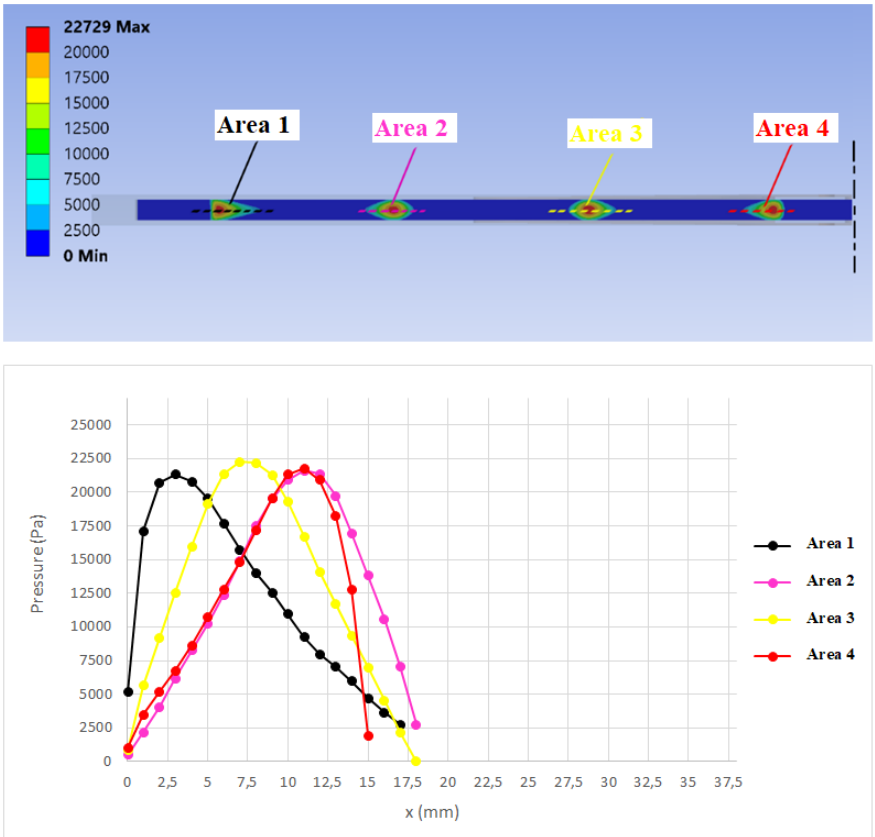

***Figure 14**. Traditional frame: distribution of significant areas of pressure and pressure trend in the four areas identified*

The maximum pressure reached is 22274 Pa, while the longitudinal extension is between 15 mm and 18 mm. The results of the Flexsys frame (Figure 15) show a symmetrical pattern in areas 2 and 3, having a similar width, while area 1 at the end of the blade, although having a greater width, has a non-symmetrical pattern. Furthermore, the maximum pressure of 26455 Pa is recorded in the area close to the centerline and is quite different from that of 15667 Pa registered in area 3. In this frame, therefore, the external force applied by the arm is not equally shared between the contact points among the frame and the blade but is mainly yield by the central area.

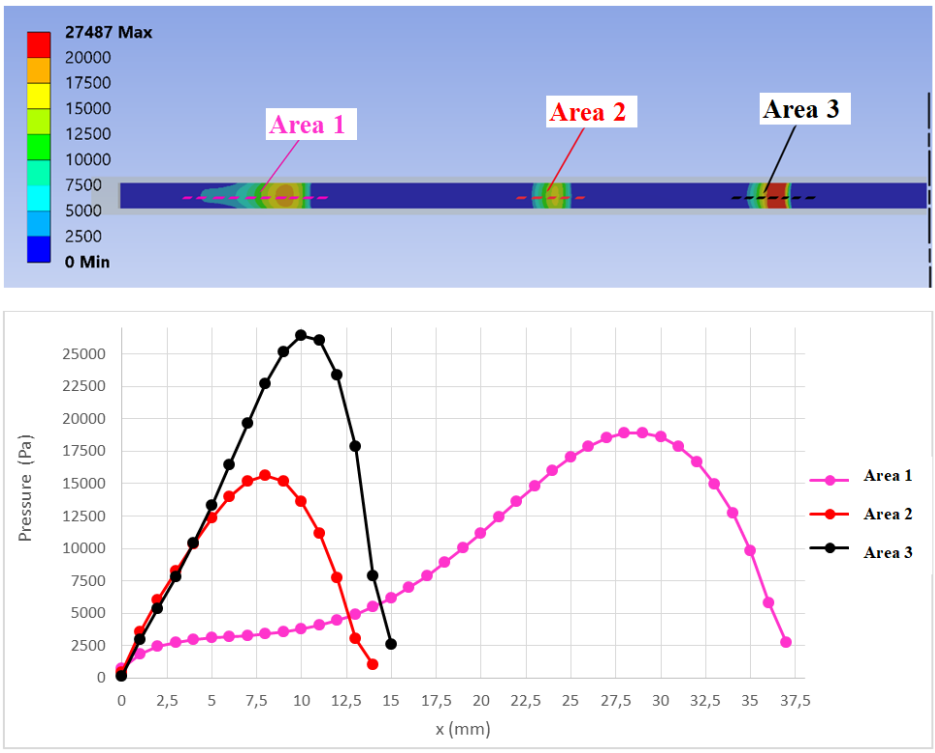

***Figure 15**. Flexsys frame: distribution of significant areas of pressure and pressure trend in the three areas identified*

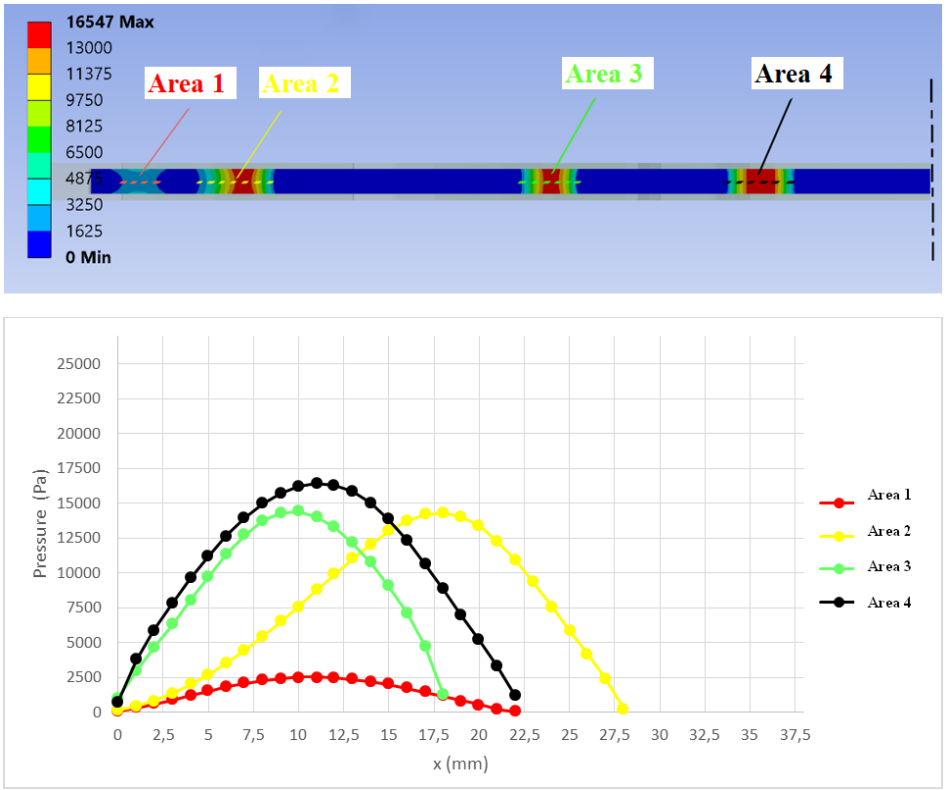

***Figure 16**. Innovative frame: distribution of significant areas of pressure and pressure trend in the four areas identified*

Finally, considering the innovative frame (Figure 16), it should be noted that, in addition to the symmetry of the pressure in the four areas, these have a greater extension than the corresponding areas of the traditional frame, reaching a width of 28 mm along the X axis. Among the three frames, therefore, the one that allows to obtain areas having almost all the same extension and pressure patterns very similar to each other is the conventional one, in which on 24.7% of the blade extension there are significant values of pressure, with a maximum percentage variation between the peaks reached in each zone equal to 4.3%. On the Flexsys chassis instead, both the extension and the pressure trend are very dissimilar between the different regions, with a variation between the maximum values present in each of them rather high, of 40.8%. Regarding instead the fraction of length of the wiper on which there are pressure values worthy of note, it is equal to 25%, substantially similar to that of the conventional frame. The innovative frame has performances, in terms of pressures trends, which are closer to those of the conventional frame. In fact, the pressure trend is substantially the same in all areas, with a percentage variation between the peaks of areas 2, 3 and 4 which is clearly smaller than that of the Flexsys frame and equal to 12.8%. With regard to the area fraction on which significant pressure values are recorded, this appears to be instead greater both than that of the conventional frame and that of the Flexsys frame, being equal to 32.7%. It is therefore able to guarantee a fairly uniform distribution of the input force between the output points and not very far from that which a conventional frame is able to ensure, but with the advantage of having a globally wider surface on which significant pressure values are applied and to be able to produce the whole structure as one-component, eliminating any assembly operation. Another aspect to pay attention to in each frame is the position of Area 1 with respect to the terminal end of the rubber. This area is the first, proceeding from the extremity towards the centerline, in which significant pressure values are recorded, therefore it is decisive to ensure that the terminal part of the wiper does not rise from the surface of the windscreen. Measuring therefore, in each of the three frames, the distance between the end of the rubber and the first point where significant pressure values are observed, it is noted that it is equal to 26 mm in the conventional frame, 25 mm in the Flexsys frame, while it is reduced to 10 mm in the innovative frame. The latter is therefore able to guarantee the application of pressure in areas closer to the extremes than the other two frames.

Providing a more uniform pressure distribution to the blade surface in contact with the windshield could also be advantageous in terms of reducing the noise and vibrations generated during the wiper operation. In fact, it can be hypothesized that the condition of maximum curvature of the windshield coinciding with the rest position of the wiper, used here as a reference configuration for the design, is also the condition in which vibrations are more likely to occur, as observed by Zolfagharian et al. [19]. The latter indeed have noticed that high vibration amplitude occurs exactly at the beginning and end of the wiper stroke while wiper lip shows almost stable motion in the middle of rotation stroke, therefore generating balanced pressures on the blade right at the beginning of its stroke could presumably determine favorable conditions by contributing to the practical multi-objective controller they developed, in order to prevent noise and vibrations in an automobile wiper system. Furthermore, limiting the possibility of generating permanent deformations in the blade by subjecting it to a quite uniform pressure, especially in its resting position with maximum curvature, could also avoid the generation of vibrations due to a deviation of the blade shape compared to its correct vertical configuration, as has been studied in depth by Lancioni et al. [20]. Moreover, comparing the weight of the three frames (Table 4) excluding the weight of the blade, it can be seen that the innovative frame, in addition to being more performing than the Flexsys one, also allows a reduction in weight compared to the latter of 16.3%.

Frames	Conventional frame	Flexsys frame	Innovative frame
Weight [g]	88	63	52.7

Table 4*. Comparison of the weights of the three frames.*

The savings achieved are even greater if we compare the innovative frame with the conventional one, compared to which the lightening is 40.1%. This is to be attributed not only to the lower density of the material used, but also to the absence of all the connecting elements between the various arches present in the conventional frame. In the analyzes carried out under rest conditions, all the structures have equally distant stresses from those of failure of the corresponding materials used while in the flexural stiffness analysis, the stress values increase more heavily for the Flexsys frame. In fact, when this structure is stressed due to the presence of the displacement and the friction between the rubber and the windshield, the stresses become significant and reach values of the order of half of the ultimate tensile strength of the material (Table 5).

Materials	**σ_{max1} [MPa]**	**σ_{max2} [MPa]**	**σ_R [MPa]**
Aluminum	68.4	-	300
PBT-GF30	23.2	60.2	130
Nylforce CF	16.9	23.4	100

Table 5*. Comparison of ultimate tensile strength (σ_R) and maximum Von Mises stress in the materials constituting the three structures (σ_{max1}= maximum Von Mises equivalent stress in the Contact pressure analysis, σ_{max2}= maximum Von Mises equivalent stress in the Flexural stiffness analysis)*

As far as fatigue resistance is concerned, there is no specific data relating to the material under examination. Similar materials, such as nylon reinforced with 30% glass fiber, show a fatigue strength of around 600000 cycles equal to about 40% of the tensile strength of the material [18].
Assuming then that the fatigue behavior of Nylforce CF is not very different from that of glass fiber reinforced nylon, the fact that in the innovative frame the stress remains below a quarter of the ultimate tensile strength, presumably ensures good resistance to fatigue of the structure at a number of cycles equal to those which a windscreen wiper frame, or about 600000 cycles, should generally withstand. The bending stiffness of the structure turns out to be quite satisfactory but can however be increased through the future use of more efficient additive manufacturing materials as well as an optimization of the geometry also in the transverse direction, in which for the moment it has been considered constant.

2.6 Prototype realization

Once satisfactory results on numerical analyzes were obtained, in order to test the operation of the frame, a Nylforce CF prototype was made using Fused Deposition Modeling technology, in which a 100% filling was set, considering the structural use of the component, and temperatures of extrusion and heating respectively of 260 °C and 65 °C. Furthermore, it has been ensured that the deposition direction of the material coincides as much as possible with the longitudinal development of the structure, so as to increase its flexural stiffness in the appropriate direction. To connect the wiper arm to the frame, the latter was equipped with an integrated structure that avoids the use of an adapter (Figure 17). Installed on a motor vehicle, the prototype performed its function excellently, cleaning the surface of the windscreen without generating streaks or other defects.

Figure 17*. Nylforce CF prototype of the innovative frame made by FDM*

4. Conclusions

It was possible to improve the performances of the single-component frame designed here, compared to those of the only other existing single-component frame, so as to obtain six areas with high pressure values towards which the input load from the arm is distributed almost uniformly, managing to guarantee performances that, although not exactly equal to those of the conventional frame, are more than sufficient for the correct functioning of the system. Integrating compliant mechanisms as a fundamental element within the proposed frame layout has allowed the wiper to adhere effectively to the windshield's maximum curvature surface while flexing without producing significant stress values in the structure, which remain lower than both other frames analyzed, thus guaranteeing adequate fatigue resistance during the expected useful life of a wiper. Generating balanced pressures on the blade's surface, also limiting the possibility of producing permanent deformations in the latter, could represent a benefit against the generation of noise and vibrations during the movement of the wiper. Towards the latter aspect, a further advantage could be related to the reduction of the distance between the extremity of the wiper and the first area of the blade where pressure is applied. This distance was in fact reduced, compared to the 26 mm of the traditional frame and the 25 mm of the Flexsys frame, to only 10 mm (Figure 16), so as to ensure greater adherence on the windshield by the blade, preventing it from lifting or creating vibrations and noise during motion.

Exploiting a combined approach to re-engineering that is able to effectively integrate the advantages offered by compliant mechanisms with the extreme production flexibility permitted by Additive Manufacturing, opens the way to new design opportunities, representing an alternative to improve certain aspects both in the production phase and in the use of a component. In the work proposed herein, in fact, reducing the number of components from 19 to 1, compared to a traditional wiper, can lead to considerable benefits on the product's time to market, eliminating the need for any assembly operation and considerably simplifying the production process as well as the inventory management to keep in stock. Furthermore, replacing a traditional multi-component metal frame with an innovative single-component nylon reinforced one, has allowed for a weight saving of 40%, a useful feature not only during the component use but also within the supply chain, allowing in fact an easier goods handling and decreasing the environmental impact, considering the reduced use of metallic materials, an aspect that makes the component's production process more sustainable.

Furthermore, the increasingly high-performance 3D printing technologies capable of using fiber-reinforced polymers (mainly carbon, glass or kevlar), extend the possibility of imagining the use of the approach here employed towards other products belonging to the automotive industry that could benefit from flexible mechanisms while maintaining the required mechanical properties.

One can think, for example, of the suspension system, the door locking mechanism, or the support structures for doors, hoods, seats and rear-view mirrors. These products, although they include different components within them, they can be analyzed according to the logic of the compliant mechanisms by geometrically break them up according to the function covered by each zone of the mechanism, since they must simultaneously resist both the application of external stresses and allow movements necessary for their correct functioning.

Exploiting the approach here used, although it's initially necessary to define through the intuition and the experience of the designer a general configuration from which to start from at least in broad lines, it is possible to refine a parameterized geometric model and improve it through numerical optimization analyzes so that, respecting the requirements and the expected performance, a lighter product can be obtained, consisting of fewer components, with low friction losses, reduced or absent lubrication, and which also allows benefits such as less use of metallic materials and a simpler logistics phase given the absence of complex assembly operations.

5. References

1. L.L. Howell , S.P. Magleby , B.M. Olsen , Handbook of Compliant Mechanisms, Wiley, Chichester, 2013
2. N. Lobontiu , Compliant Mechanisms: Design of Flexure Hinges, CRC Press, Boca Raton and Fla., 2003
3. J. Beroz , S. Awtar , M. Bedewy , S. Tawfick , A.J. Hart , Compliant microgripper with parallel straight-line jaw trajectory for nanostructure manipulation, in: Proceedings of the Twenty-sixth Annual Meeting of the ASPE, 2011
4. R. Bharanidaran, T. Ramesh, A modified post-processing technique to design a compliant based microgripper with a plunger using topological optimization, Int. J. Adv. Manuf. Technol. 93 (2017) 103–112. https://doi.org/10.1007/s00170-015-7801-z.
5. I. Ivanov, B. Corves, Stiffness-oriented design of a flexure hinge-based parallel manipulator, Mech. Based Des. Struct. Mach. 42 (2014) 326–342. https://doi.org/10.1080/15397734.2014.899913.
6. S. Bütefisch, V. Seidemann, S. Büttgenbach, Novel micro-pneumatic actuator for MEMS, Sensors Actuators, A Phys. 97–98 (2002) 638–645. https://doi.org/10.1016/S0924-4247(01)00843-3.
7. R. Keoschkerjan, H. Wurmus, A novel microgripper with parallel movement of gripping arms, Proc. 8th Int. Conf. New Actuators. (2002) 321–324.
8. W. Liu, J.K. Mills, MEMS remote centre of compliance design, 2006 IEEE Int. Conf. Mechatronics Autom. ICMA 2006. 2006 (2006) 118–123. https://doi.org/10.1109/ICMA.2006.257463.
9. V. Yakovlevich Prinz, V. Alexandrovich Seleznev, A. Victorovich Prinz, A. Vladimirovich Kopylov, 3D heterostructures and systems for novel MEMS/NEMS, Sci. Technol. Adv. Mater. 10 (2009). https://doi.org/10.1088/1468-6996/10/3/034502.
10. H.H. Pham, I.M. Chen, Evaluation of resolution of flexure parallel mechanisms for ultraprecision manipulation, Rev. Sci. Instrum. (2004) 3016-3024 https://doi.org/10.1063/1.1786351.
11. M. Verotti, A. Dochshanov, N.P. Belfiore, Compliance Synthesis of CSFH MEMS-Based Microgrippers, J. Mech. Des. Trans. ASME. (2017). https://doi.org/10.1115/1.4035053.
12. Z. Hongzhe, B. Shusheng, P. Bo, Dynamic analysis and experiment of a novel ultra-precision compliant linear-motion mechanism, Precis. Eng. 42 (2015) 352–359. https://doi.org/10.1016/j.precisioneng.2015.06.002.
13. M. Torralba, J.A. Yagüe-Fabra, J.A. Albajez, J.J. Aguilar, Design optimization for the measurement accuracy improvement of a large range nanopositioning stage, Sensors (Switzerland). 16 (2016). https://doi.org/10.3390/s16010084.
14. C. Zhao, M.H. Montaseri, G.S. Wood, S.H. Pu, A.A. Seshia, M. Kraft, A review on coupled MEMS resonators for sensing applications utilizing mode localization, Sensors Actuators, A Phys. 249 (2016) 93–111. https://doi.org/10.1016/j.sna.2016.07.015.
15. Kota, Herrick, Compliant windshield wiper systems, *United States Patents 2006/0213020 A1*, (2006).
16. S. Cadirci, S.E. Ak, B. Selenbas, H. Gunes, Numerical and experimental investigation of wiper system performance at high speeds, J. Appl. Fluid Mech. 10 (2017) 861–870. https://doi.org/10.18869/acadpub.jafm.73.240.26527.

17. G. Bódai, T.J. Goda, Sliding friction of wiper blade: Measurement, FE modeling and mixed friction simulation, Tribol. Int. 70 (2014) 63–74. https://doi.org/10.1016/j.triboint.2013.07.013.
18. Esmaeillou, Ferreira, Bellenger, Tcharkhtchi, Fatigue behavior of polyamide 66/glass fiber under various kinds of applied load, *Polymer Composites*, pag 540-547, (2012).
19. A. Zolfagharian, A. Noshadi, M.Z.M. Zain, A.R.A. Bakar, Practical multi-objective controller for preventing noise and vibration in an automobile wiper system, Swarm Evol. Comput. 8 (2013) 54–68. https://doi.org/10.1016/j.swevo.2012.08.004.
20. G. Lancioni, S. Lenci, U. Galvanetto, Dynamics of windscreen wiper blades: Squeal noise, reversal noise and chattering, Int. J. Non. Linear. Mech. 80 (2016) 132–143. https://doi.org/10.1016/j.ijnonlinmec.2015.10.003.